Int. j. inf. tecnol. (May 2022) 14(3):1455–1465
https://doi.org/10.1007/s41870-021-00652-8

ORIGINAL RESEARCH

Isotherm recognition on a V-notch specimen by color identification method

P. L. Rupesh[1] · **M. Arulprakasajothi**[1] · **K. Raja**[1]

Received: 27 September 2020 / Accepted: 24 March 2021 / Published online: 8 April 2021

Abstract In routine existence, the utilization of vehicles is increasing in a enormous way among the people. This leads to the production of vehicles in a high rate. The engine parts used for the proper functioning of the vehicles needs a extreme care. These parts are subjected to extreme load and stress. As the engine produces work used to move the vehicles due to the combustion of fuel taking place inside the parts, they are subjected to high thermal stress (or) high temperature. The temperature at which the part elongates should be determined before the parts are incorporated inside the engine. The parts can be subjected to heat flow equal to one that is produced during combustion and the temperature gradient on the surface of the engine part can be calibrated. The present work concentrates on the experimental recognition of the temperature gradient on the surface of a V-notch specimen. The experimental recognition has been done by the utilization of a special paint which changes its color as subjected to temperature rise. The colors obtained from the experimental observation has been verified by two color identification methods. The color identification methods and the experimental results were hold in good agreement.

Keywords Temperature · Color contour · RGB · Hue · Light

✉ P. L. Rupesh
1rupeshkumar221@gmail.com

[1] Department of Mechanical Engineering, Veltech Rangarajan Dr Sagunthala R & D Institute of Science and Technology, Chennai, India

1 Introduction

In the emerging era of the industries and vehicles, heat energy produced due to combustion of fuels play a vital role. The proper maintenance of the components used for the extraction of heat (combustion) is too essential. A high temperature exothermic redox chemical reaction takes place between the fuel and the oxidant is called as Combustion. The reaction becomes self-sustained because of the sufficient energy provided by the heat from a flame produced during combustion. The thermal energy transferred across a well-defined boundary around a thermodynamic system is called as heat [1, 2]. This energy is transferred between systems through three modes called as (a) conduction; (b) convection and (c) radiation. If the heat is transferred through an intervening matter such as solid (e.g. block of metal), then the mode is called as conduction. The basic principle in this mode is that both surfaces of the solid should be at different temperatures (one at a high temperature and other at a lower temperature). If the transfer of heat takes place due to a flowing fluid (gas or liquid), then the mode of transfer is called as Convection. The transmission of heat energy through space (or) vaccum without the intervention of any physical matter is called as Radiation [3, 4].

In most of the automotive sectors, internal combustion (IC) engine is employed to produce the mechanical work from the process of combustion. The basic components/parts of the IC engine have been indicated as shown in Fig. 1.

The combustion process responsible for the production of work as shown in Fig. 2, produces enormous heat energy. The heat energy is exhibited as a flame with a high temperature of around 850 °C [5]. The flame produced exhibits high temperature to the engine parts. The parts of

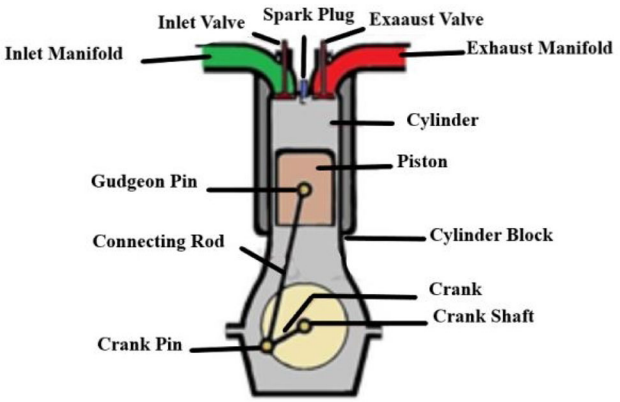

Fig. 1 Basic components of internal combustion engine

the engine subjected to high temperature has been indicated in Fig. 2.

Piston crown, Intake manifold, exhaust manifold, inlet valve and exhaust valve are the engine parts exposed to high temperature flame [4]. Among these parts, piston crown is exposed more to the flame as the combustion takes place on the top of piston crown. Due to the enormous heat energy, piston has been subjected to high heat load, which means the piston crown exposed to variable temperature gradient.

The need to limit the measure of air utilized in liner film cooling and along these lines diminish the yield of carbon monoxide and unburned hydrocarbons has been identified by D.

Ballal et al. [5] to develop familiarity with toxin outflows from gas turbine engines. An examination has been made of trial information acquired on a uniquely structured film-cooling rig which has prompted the improvement of a computation technique for liner divider temperatures within the sight of film cooling the examination of Chen et al. [6] proposes an improved micro combustor with a rectangular rib to improve the temperature level of the combustor divider. In addition, the OH mass portion, temperature conveyance, and external divider temperature of the first and improved combustors of premixed hydrogen/air blazes are numerically examined under different bay speeds and comparability proportions. The results observed by the author shows that the improved micro combustor upgrades heat move between the blend and divider since its distribution zone is bigger than that of the first, along these lines bringing about high divider temperature. On the other hand, warm opposition in the flat heading increments with upstream and downstream advance lengths. Thusly, the external divider temperature diminishes with step length in the improved combustor. A high identicalness proportion (e.g., 0.6) may bring about the pulverization of the combustor in light of the fact that the divider temperature has surpassed the satisfactory temperature of divider material quartz. Therefore, it was finalized from the experiment that the improved micro combustor is suggested for miniaturized scale thermophotovoltaic frameworks. Namayandeh et al. [7] examined the temperature dispersion of clay boards for a V94.2 gas turbine combustor exposed to sensible activity conditions is introduced utilizing three-dimensional limited contrast technique. A rearranged model of alumina clay is utilized to acquire the temperature appropriation. The outside warm loads comprise of convection and radiation heat moves are viewed as that these heaps are applied to level fragmented board on hot side and constrained convection cooling on the opposite side. First the temperatures of hot and cold sides of earthenware are determined. At that point, the warm limit states of all other fired sides are assessed by the field perceptions. At long last, the temperature disseminations of earthenware boards for a V94.2 gas turbine combustor are registered by MATLAB software. The experimental outcomes show that the gas emissivity for dissemination mode is more than premix thusly the radiation heat motion and temperature will be more. The aftereffects of this work are approved by ANSYS and ABAQUS virtual products. It is demonstrated that there is a

Fig. 2 Parts exposed to flame

decent understanding between all outcomes. Norgren [1] has calculated the liner temperature dependent on a consistent state radiative and convective warmth balance at the liner divider. It was found that the determined liner temperature were around 8 percent higher than test esteems. A radiometer was utilized to tentatively decide estimations of fire temperature and fire emissivity. Film cooling viability was determined from an observational tempestuous blending articulation accepting a fierce blending level of 2 percent. Liner divider temperatures were assessed in a rectangular combustor piece 15 by 30 cm (6 by 12 in.) and attempted at pressures up to 26.7 atm and delta temperatures up to 922 K (1660°R).

The inferences drawn from the above literatures' states that temperature detection on the surface of the parts of the engine is too essential. The current study deals with the application of special solvent-based paint on the surface to detect the temperature gradient through change in color. A user-friendly and cost-effective method has been projected in this study for thermal profiling of components as the selection of materials for the manufacturing of engine parts depends on the detection of permissible temperature range allowed based on the material of the component.

2 Design and fabrication of specimen

A specimen of varying cross section has been designed and the model has been shown in Fig. 3. The model depicted in Fig. 3. manifests that the area of the model was large at beginning and start to reduce up to a certain point and it starts increasing from that point. The center portion of the sample where it contracts and expands is called as throat. Figure 3a depicts the three-dimensional model of the specimen created using designing software package. The dimensions of the model have been projected in the Fig. 3b.

The specimen has been fabricated using mild steel (or) low carbon steel and the fabricated specimen has been coated with solvent-based paint as shown in Fig. 4a, b. The holes have been projected to hold the specimen for the experimentation purpose.

The chemical composition of the carbon steel used for the specimen fabrication has been listed in Table 1. The content of manganese is higher (0.7–0.9%) and it exhibits good thermal properties which indicates that the material chosen for fabrication can withstand high temperature.

3 Experimentation

The fabricated model after the coating of paint has been exposed to a flame originating from the butane torch. The heating is continued for nearly 30 min. The specimen undergoes a drastic color change as shown in Fig. 5. From the human vison, it was evident that at the center portion of the specimen, a distinct color has been observed. The right and left side of the specimen undergoes different color changes than the color at the center. It was also observed that the color changes on both sides of the center are same.

From Fig. 5, it was observed that the color at the mid of the specimen is blue, the other colors on both sides are yellow, brown and red based on human vision of color indication. It is mandatory to match these colors with the temperature values in order to get the temperature gradient on the surface of the specimen. This can be achieved by comparing these colors with a calibration data. The following ASTM methods shown in Table 2 has been employed in the current study for evaluation of color obtained and other influencing properties [8].

3.1 Calibration database

The calibration database is formed through warm up of square specimens of size 1 mm × 2 mm under different temperatures in a furnace. As the temperature increases, the color of the square specimen changes, therefore for each temperature, a distinct color is observed on the specimen.

The observed color contour can be compared with the color of the square specimen shown in Fig. 6 to obtain the value of temperature corresponding to the color as in calibration data.

3.2 Color attributes

The colors can also be predicted with the help of its attributes such as RGB and HSV according to ASTM E805 and ASTM E991. Colors arises from the mixing of three primary colors red, green and blue [9]. The method of color identification using the mixing pattern is called as RGB method. The RGB value of each square specimen has been determined using a image processing algorithm.

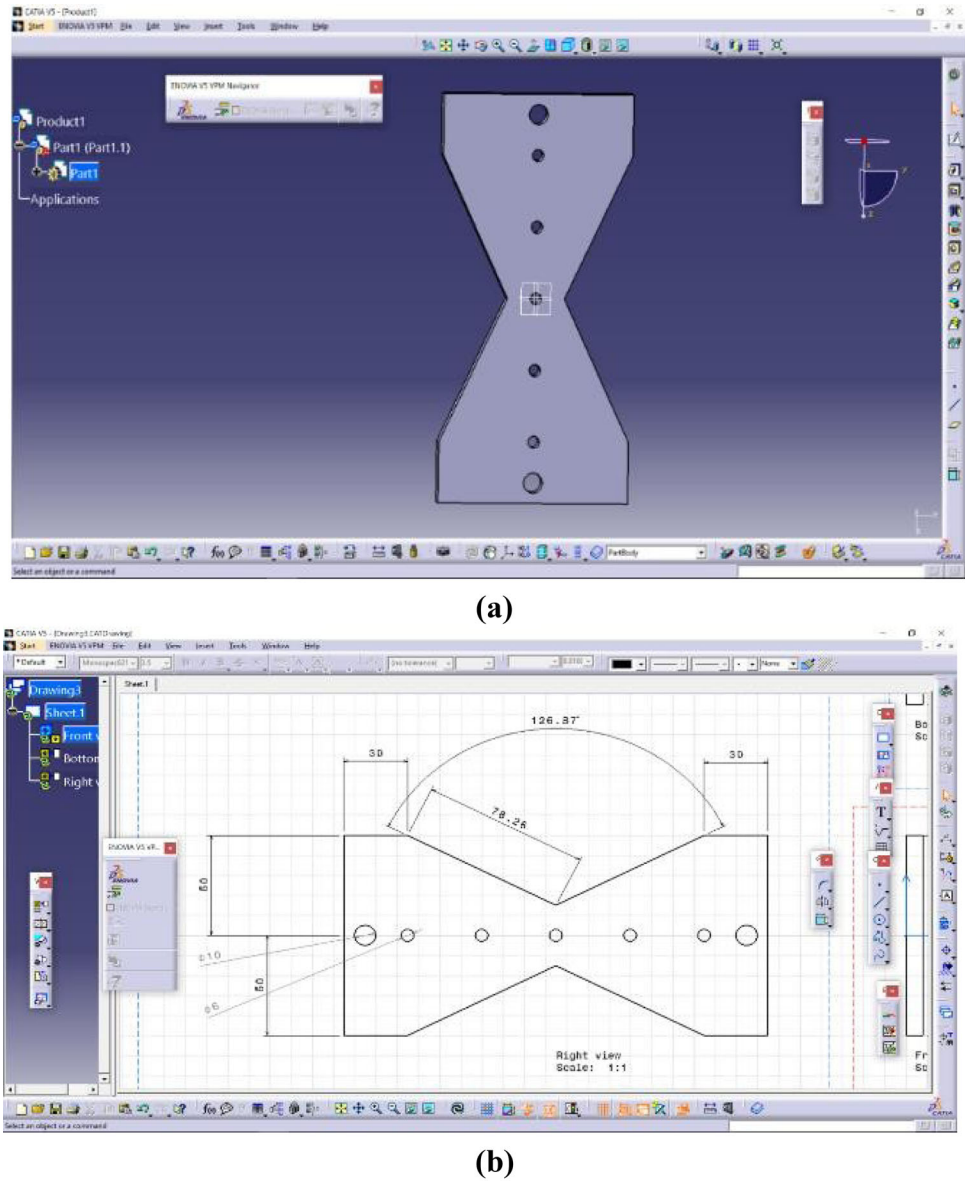

Fig. 3 V-notch specimen. **a** 3D model; **b** 2D drafting

```
from PIL import Image
import cv2
im = Image.open('D:/Square Specimen.jpeg')
s = cv2.imread('D:/ Square Specimen.jpeg')
h, w, c = s.shape
rgb_im = im.convert('RGB')
r, g, b = rgb_im.getpixel((w-1, h-1))
print(r, g, b)
```

The algorithm used for the determination of RGB value has been projected above. The determined RGB values for the square specimens at different temperature and color has been depicted in below Table 3.

The color codes of the colors existing in calibration data base was also indicated in Table 4. The values of RGB obtained from the algorithm for the square specimens at different colors has been depicted in Fig. 7.

3.3 HSV method

The colors can also be identified by using the properties of color such as hue, saturation and lightness [8, 10, 11]. The predominant color existing in the color obtained will be provided by Hue [9]. The saturation of the color indicates the percentage of saturation in the color. The percentage of luminescence is given by the factor lightness. The properties of color have been indicated in Fig. 8.

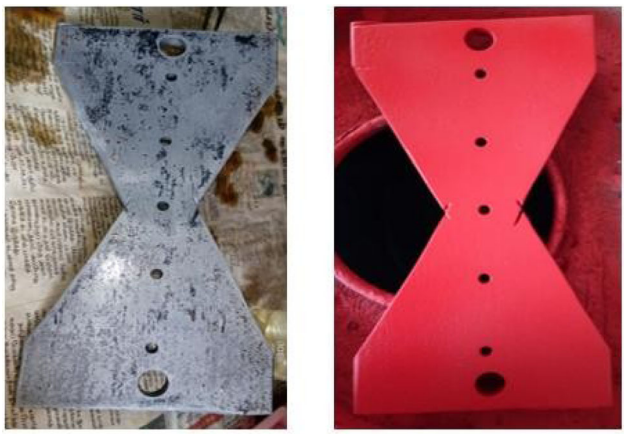

(a) (b)

Fig. 4 V-notch specimen. **a** Fabricated; **b** painted

Table 1 Chemical composition

Composition	% Content
Carbon	0.16–0.18
Silicon	0.4
Manganese	0.7–0.9
Sulphur	0.04
Phosphorous	0.04

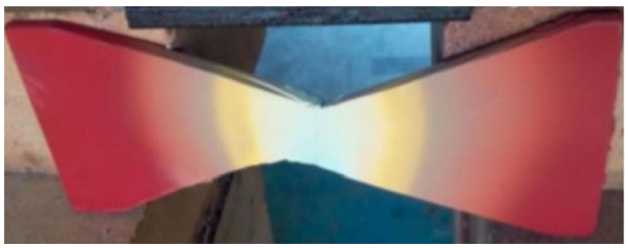

Fig. 5 Color contours of V-notch specimen

4 Results and discussion

4.1 RGB vs. temperature

The values of RGB obtained from the algorithm for the square specimens at different colors has been depicted in the form of graph as shown in Fig. 8 in order to observe the variation of the color attributes [10] with respect to temperature.

The graph depicted in Fig. 9 reveals that the value of red (R) was higher at the initial temperature and as the temperature increases, the value of R decreases. It is also observed that the value of green (G) and blue (B) was at low at initial temperature and as the temperature increases, the value of G and B increases. The initial color of the paint was red but with increase in temperature the color changes to green (i.e.) In the RGB value, the value of green becomes higher at temperature of 850 °C.

4.2 Detection of Temperature in V-notch specimen

Based on the data provided by Fig. 9, the color obtained on the surface of the specimen can be easily matched with the value of temperature. The combination of RGB values can be predicted from the V-notch specimen surface based on the algorithm provided in the section of color attributes.

Figure 10 depicts the value of RGB at the particular points available on the specimen surface. The data available in Fig. 10 does not exactly matches with the RGB values of the square specimens. The obtained RGB values on the V-notch specimen lies between the range of the RGB values shown in Table 3.

The temperature range over the specimen surface can be detected using the value of RGB obtained as shown in Fig. 11, The exact temperature cannot be visualized due to the inexact value of RGB values,

Table 2 ASTM standards

ASTM standard	Applications	Description
ASTM D2244	Standard practice for calculation of color tolerances and color differences from instrumentally measured color coordinates	Describes the calculation of rectangular and elliptical color differences for opaque samples
ASTM E805	Standard practice for identification of instrumental methods of color or color difference measurement of materials	Describes how to effectively communicate color values and all the parameters that affect them
ASTM E991	Standard practice for color measurement of fluorescent specimens	Describes measurement of fluorescent samples and presenting numerically how they appear in daylight
ASTM E1347	Standard test method for color and color-difference measurement by tristimulus (filter) colorimetry	Describes color measurement using tristimulus colorimeters of either 45°/0° or diffuse geometry

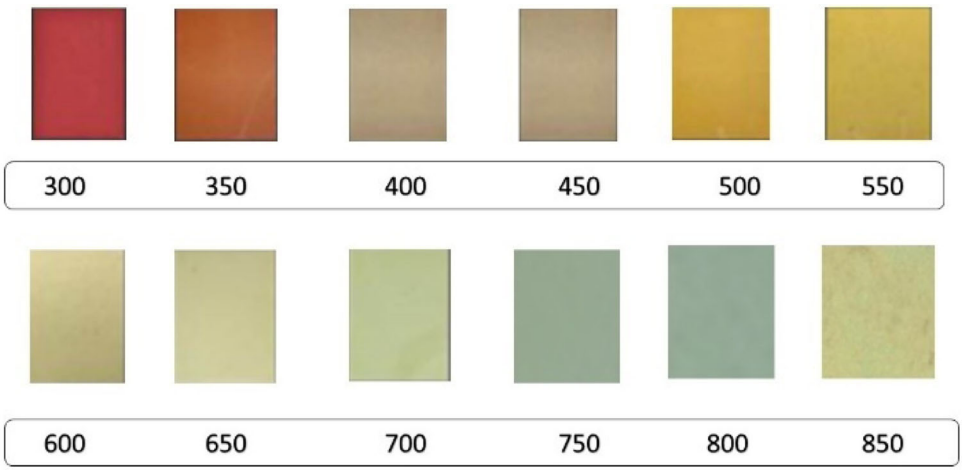

Fig. 6 Color change with temperature

Table 3 RGB and color code

Temperature (°C)	R	G	B	Colour code
300	184	65	69	#B84145
350	185	111	64	#B96F40
400	180	150	117	#B49675
450	186	168	132	#BAA884
500	209	169	73	#D1A949
550	211	182	80	#D3B650
600	205	193	143	#CDC12B
650	205	201	153	#CDC999
700	189	198	153	#BDC699
750	150	168	144	#96A890
800	148	169	150	#94A996
850	180	180	156	#B4B49C

Table 4 RGB to HSL conversion

Steps	Description	Formulae	
Step 1	Determination of R′, G′ and B′	$R' = \frac{R}{255},\ G' = \frac{G}{255},\ B' = \frac{B}{255}$	
Step 2	Determination of C_{max} and C_{min}	$C_{max} = \max(R',\ G',\ B'),\ C_{min} = \min(R',\ G',\ B')$	
Step 3	Determination of Δ	$\Delta = C_{max} - C_{min}$	
Step 4	Determination of hue (H)	$\Delta = 0$	$H = 0$
		C_{max} = R’	$H = 60^\circ \times \left(\frac{G'-B'}{\Delta}\right)$
		C_{max} = G’	$H = 60^\circ \times \left(\frac{B'-R'}{\Delta}\right) + 2$
		C_{max} = B’	$H = 60^\circ \times \left(\frac{R'-G'}{\Delta}\right) + 4$
Step 5	Determination of saturation (S)	$\Delta = 0$	$S = 0$
		$\Delta < > 0$	$S = \frac{\Delta}{1-\lvert 2L-1\rvert}$
Step 6	Determination of lightness (L)	$L = \frac{C_{max}+C_{min}}{2}$	

Fig. 7 RGB of square specimens

The temperature range is not acceptable to detect the effect of heat on the engine parts. The exact value of temperature is needed. The exact value may be determined based on the conversion of RGB into HSL. Even though, the observed color is a mixture of several colors, one of the color property Hue depicts the dominant color in it with a prescribed value [8]. The saturation and lightness of the color is also important in the detection of color [8, 10]. Several factors such as object shape, illumination geometry and the properties of reflectance such as hue, value and lightness influence the appearance of color observed on the surface of objects [10].

4.3 RGB to HSL conversion

In order to detect the exact temperature on the heated specimen, the observed RGB values should be converted to HSL. Table 4 lists out the steps and formulae to convert RGB into HSL.

The converted values of HSL and the corresponding RGB and temperature values has been tabulated in Table 5.

The calculated HSL values have been plotted with temperature to determine the effect of temperature on Hue. The graph depicted in Fig. 12 shows that the value of Hue increases with increase in Temperature from 350^0C up to 800^0C. After that, the value of Hue decreases for 850 °.

From the trend obtained in graph, it is evident that each temperature value is associated with a distinguished color with separate hue value. Based on the Hue value, the values of temperature has been plotted on the V-notch specimen surface as shown in below Fig. 13. The coating applied to the surface has a peculiar property is that the coating changes its color when it has been elevated to temperature change [12]. It has been clearly evident from [10, 13], the

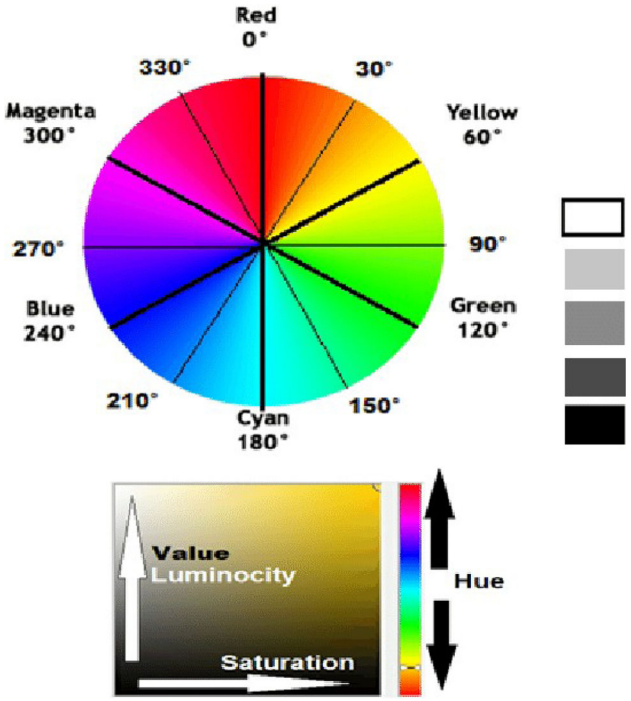

Fig. 8 HSL representation

color depends on the property Hue and it has greater influence. The coating molecules were excited to a certain wavelength when it has been exposed to certain temperature [11, 14] due to the property of reflectance. It has been also proven that the wavelength of the respective color and its property Hue has a very close relationship [8, 9, 11, 13]. In this way, temperature is connected to the Hue property

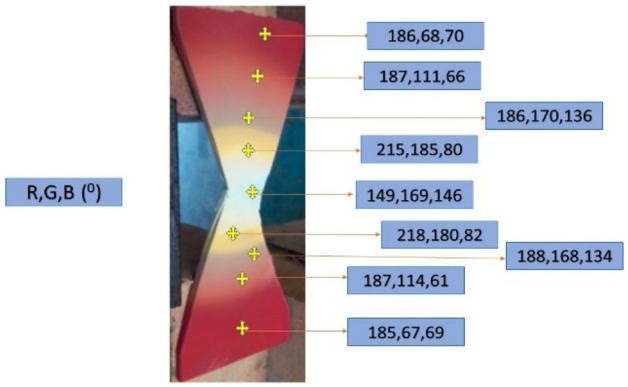

Fig. 10 RGB of V-notch specimens

and it has been visualized from the graph depicted in Fig. 12.

4.4 Isotherm lines on the specimen

Based on the temperature values obtained through the values of hue, the temperature at each point of the surface has been plotted as shown in below Fig. 14.

The isotherms have been plotted based on the above graph. The area under a certain temperature has been divided from other temperature values and a boundary is created [7]. This sort of boundary creation based on the values of temperature is called as isotherms. The isothermal lines were plotted as shown in below Fig. 15.

Fig. 9 RGB and temperature

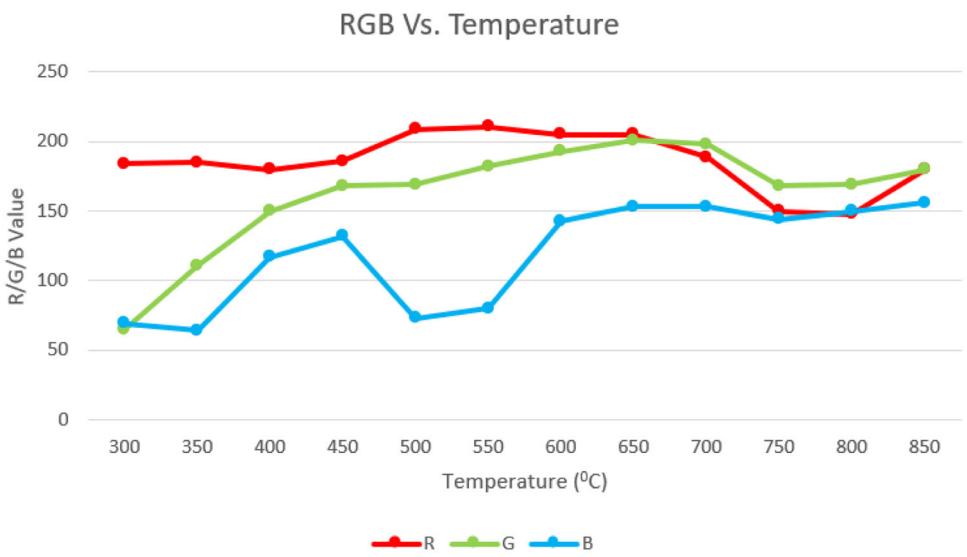

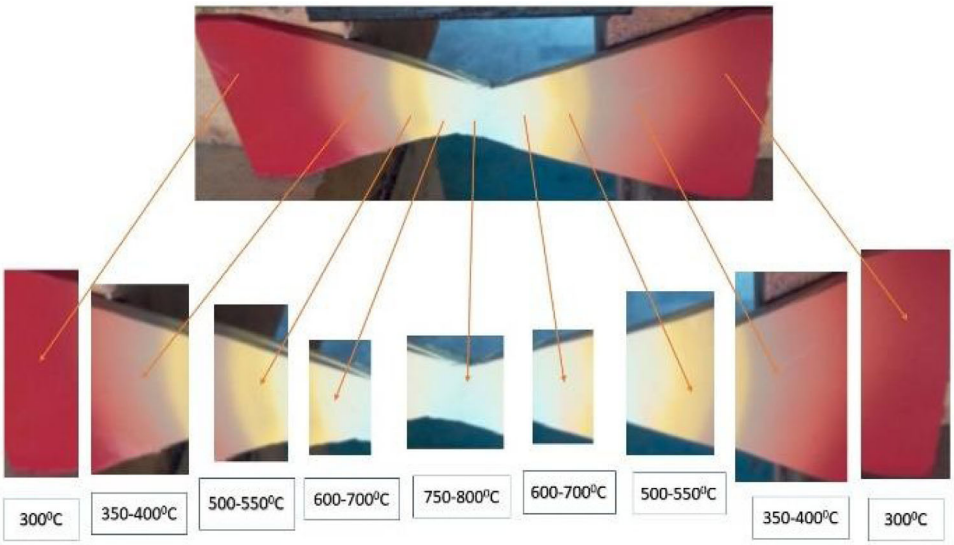

Fig. 11 Temperature range

Table 5 HSL values

Temperature(^{0}C)	R	G	B	H	S	L
350	185	111	64	23	49	49
400	180	150	117	31	30	58
450	186	168	132	40	28	62
500	209	169	73	42	60	55
550	211	182	80	47	60	57
600	205	201	153	55	34	70
650	205	193	143	56	65	49
700	189	198	153	72	28	69
750	150	168	144	105	12	61
800	148	169	150	126	11	62
850	180	180	156	58	33	65

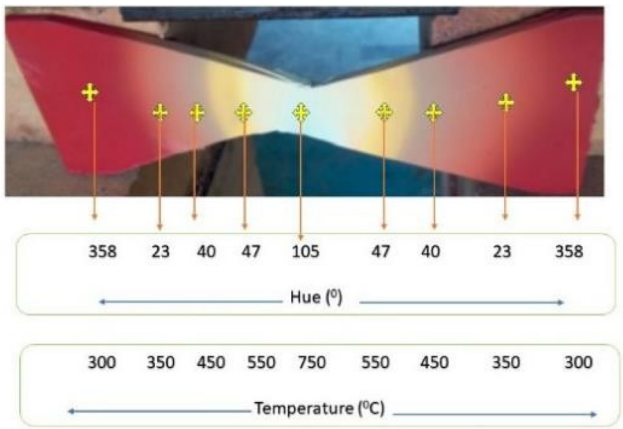

Fig. 13 Hue and temperature

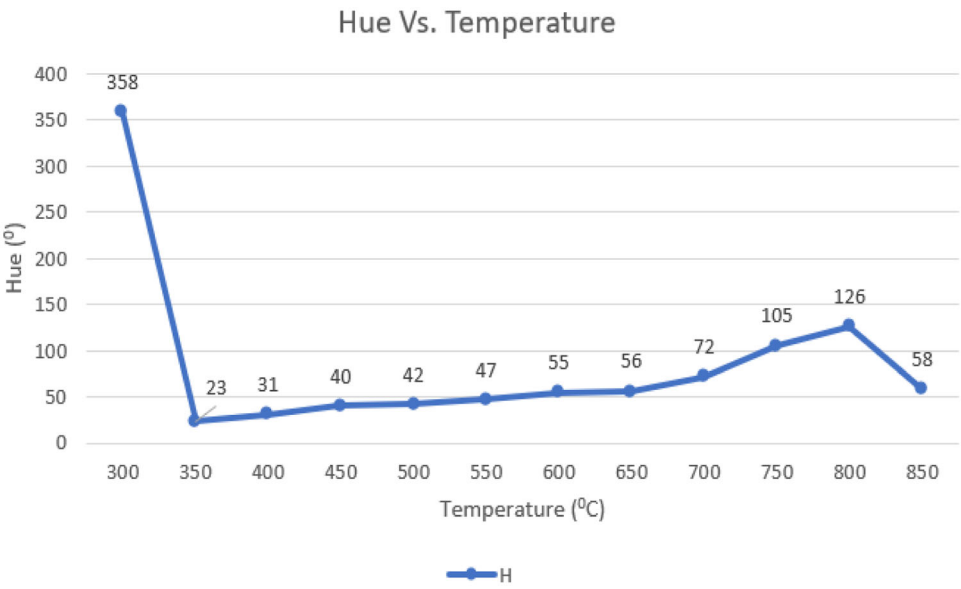

Fig. 12 Variation of hue and temperature

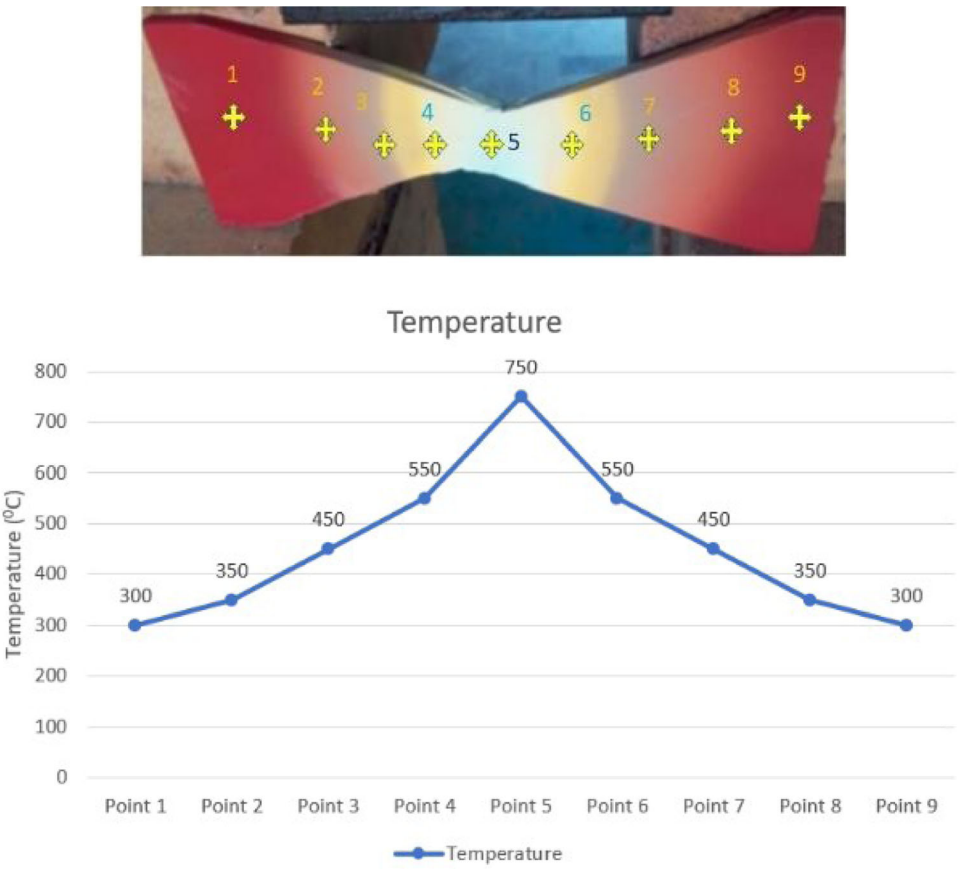

Fig. 14 Temperature detection

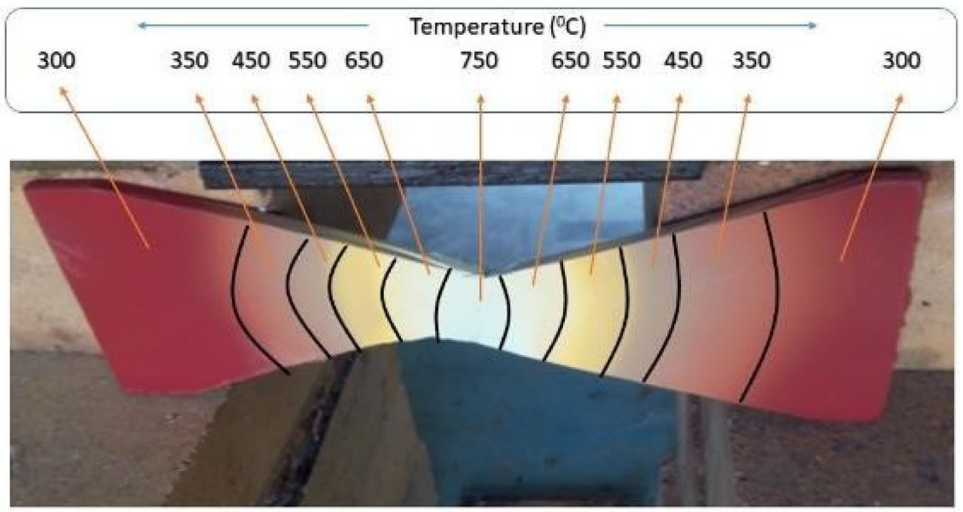

Fig. 15 Isotherm

5 Conclusion

The experimental recognition of the temperature gradient on the surface of a V-notch specimen has been done. The experimental recognition has been performed by the utilization of a special paint which changes its color as subjected to temperature rise. The colors obtained from the experimental observation has been verified by RGB and HSL method. The color identification methods and the experimental results were hold in good agreement. The temperature on the specimen surface has been identified by the color using Hue property. The isotherms were identified and drawn on the specimen surface. The results observed from the study reveals that the usage of this special paint pays a greater involvement in prediction of temperature variation on the surface of hot specimen. Now a days,

selection of suitable materials for the fabrication of gas turbine components has been a challenging task, therefore the color recognition method proposed in the above work has been planned to be implemented in gas turbine industries as a part of future work .

References

1. NorgrenCT (1973) Comparison of primary-zone combustor liner wall temperatures with calculated predictions. NASA Technical Memorandum
2. Wilhelmsson C, Vressner A, Tunestal P, Johansson B (2005) Combustion chamber wall temperature measurement and modeling during transient HCCI operation. SAE Technical Paper Series
3. Wan J, Fan A, Yao H (2016) Effect of the length of a plate flame holder on flame blowout limit in a micro-combustor with preheating channels. Combust Flame 170:53–62
4. Wang Y, Zhou J, Zhao Q, Yang W, Zhou J, Zhang Y (2017) Comparison of catalytic combustion of methane and n-butane in microtube. CIESC J 68:896–902
5. BallalDR, Lefebvre AH (1973) A proposed method for calculating film-cooled wall temperatures in gas turbine combustion chamber. Cranfield Report SME No. 4
6. Chen H, Liu W (2019) Numerical investigation of the combustion in an improved microcombustion chamber with rib. J Chem
7. Namayandeh MJ, Mohammadimehr M, Mehrabi M (2019) "Temperature distribution of ceramic panels of a V94.2 gas turbine combustor under realistic operation conditions. Adv Mater Res 8(2):117–135
8. (2006) "Test methods for color measurement", applications note, insight on color. Hunter Lab 18(4):1
9. Becker D (2016) Color measurement. In: Chapter 37, color trends and selection for product design. Plastics Design Library, pp 179–182 (2016)
10. Giesel M, Gegenfurtner KR (2010) Color appearance of real objects varying in material, hue, and shape. J Vis 10(9):1–2
11. BullettTR (1999) Appearance qualities of paint—basic concepts. In: Chapter 17, paint and surface coatings (Second edition)-theory and practice. Woodhead Publishing Series in Metals and Surface Engineering, pp 621–641
12. Yilmaz H, Cam O, Yilmaz I (2017) Effect of micro combustor geometry on combustion and emission behavior of premixed hydrogen/air flames. Energy 135:585–597
13. Arulprakasajothi M, Rupesh PL (2020) Surface temperature measurement of gas turbine combustor using temperature-indicating paint. Int J Ambient Energy. https://doi.org/10.1080/01430750.2020.1731709
14. Rupesh PL, Prakasajothi A (2021) Thermal distribution on gas turbine blade using thermal paint. In: Innovative design, analysis and development practices in aerospace and automotive engineering, lecture notes in mechanical engineering, pp 101–113